The raw starch binding domain of cyclodextrin glycosyltransferase from Bacillus circulans strain 251

Penninga, Dirk; Veen, Bart A. van der; Knegtel, Ronald M.A.; Hijum, Sacha A.F.T. van; Rozeboom, Henriëtte J.; Kalk, Kor H.; Dijkstra, Bauke W.; Dijkhuizen, Lubbert

Published in:
The Journal of Biological Chemistry

DOI:
10.1074/jbc.271.51.32777

THE JOURNAL OF BIOLOGICAL CHEMISTRY
Vol. 271, No. 51, Issue of December 20, pp. 32777–32784, 1996

Printed in U.S.A.

The Raw Starch Binding Domain of Cyclodextrin Glycosyltransferase from *Bacillus circulans* Strain 251*

(Received for publication, January 22, 1996, and in revised form, October 4, 1996)

Dirk Penninga‡§, Bart A. van der Veen‡§, Ronald M. A. Knegtel¶, Sacha A. F. T. van Hijum¶, Henriëtte J. Rozeboom¶, Kor H. Kalk¶, Bauke W. Dijkstra¶, and Lubbert Dijkhuizen‡‖

From the ‡Department of Microbiology, Groningen Biomolecular Sciences and Biotechnology Institute (GBB), University of Groningen, Kerklaan 30, 9751 NN Haren, The Netherlands and the ¶BIOSON Research Institute and Laboratory of Biophysical Chemistry, Groningen Biomolecular Sciences and Biotechnology Institute (GBB), University of Groningen, Nijenborgh 4, 9747 AG Groningen, The Netherlands

The E-domain of cyclodextrin glycosyltransferase (CGTase) (EC 2.4.1.19) from *Bacillus circulans* strain 251 is a putative raw starch binding domain. Analysis of the maltose-dependent CGTase crystal structure revealed that each enzyme molecule contained three maltose molecules, situated at contact points between protein molecules. Two of these maltoses were bound to specific sites in the E-domain, the third maltose was bound at the C-domain.

To delineate the roles in raw starch binding and cyclization reaction kinetics of the two maltose binding sites in the E-domain, we replaced Trp-616 and Trp-662 of maltose binding site 1 and Tyr-633 of maltose binding site 2 by alanines using site-directed mutagenesis. Purified mutant CGTases were characterized with respect to raw starch binding and cyclization reaction kinetics on both soluble and raw starch. The results show that maltose binding site 1 is most important for raw starch binding, whereas maltose binding site 2 is involved in guiding linear starch chains into the active site. β-Cyclodextrin causes product inhibition by interfering with catalysis in the active site and the function of maltose binding site 2 in the E-domain.

CGTase mutants in the E-domain maltose binding site 1 could no longer be crystallized as maltose-dependent monomers. Instead, the W616A mutant CGTase protein was successfully crystallized as a carbohydrate-independent dimer; its structure has been refined to 2.2 Å resolution. The three-dimensional structure shows that, within the error limits, neither the absence of carbohydrates nor the W616A mutation caused significant further conformational changes. The modified starch binding and cyclization kinetic properties observed with the mutant CGTase proteins thus can be directly related to the amino acid replacements.

Cyclodextrin glycosyltransferase (CGTase, EC 2.4.1.19) converts raw starch into cyclodextrins, which are cyclic oligomers of α(1→4) linked glucose residues (1, 2). Cyclodextrins can form inclusion complexes with small hydrophobic molecules (3) and are increasingly used in industrial and research applications (4). The *cgt* gene of *Bacillus circulans* strain 251 has been cloned and sequenced, and the crystal structure of the CGTase protein has been determined at 2.0 Å resolution (1, 5). The protein consists of a single polypeptide chain of 686 amino acid residues; as in other known CGTase structures (6–8), five domains (A–E) can be recognized. The three N-terminal domains (A–C) have structural similarity with the three α-amylase domains. Domain E contains a raw starch binding motif (5, 9, 10) (see Fig. 1).

In glucoamylases, several Trp residues (Trp-590, Trp-615) in the domain containing this motif were shown to be essential for degradation of raw starch (11–13). This domain also has a high affinity for β-cyclodextrin (14, 15), the binding of which inhibits starch hydrolysis (16). Also in CGTases, a starch binding site separate from the active site is present (17), and fusion of the E-domain of the *Bacillus macerans* CGTase to β-galactosidase demonstrated that it can function as a starch binding domain (18). CGTase is sensitive to product inhibition by cyclodextrin, which severely limits yields in industrial production processes (19). Recently, we showed that cyclodextrins bind at the CGTase E-domain (20). This suggested that cyclodextrins may interfere with starch binding.

Here we report a detailed analysis of raw starch binding and cyclization reaction kinetics of wild-type and mutant CGTase enzymes with a modified E-domain. Evidence is presented that the E-domain functions in binding of raw starch and guiding of linear starch chains into the active site.

EXPERIMENTAL PROCEDURES

Bacterial Strains and Plasmids—Escherichia coli MC1061 (M*hsd*R *mcr*B *ara*D139 Δ(*ara*ABC-*leu*)7679 Δ*lac*X74 *gal*U *gal*K *rps*L *thi*) (21) was used for recombinant DNA manipulations and site-directed mutagenesis. *E. coli* DH5α (F′/*end*A1 *hsd*R17 *sup*E44 *thi*1 *rec*A1 *gyr*A (Nal^r) *rel*A1 (*lac*ZYA-*arg*F) U196 (ø80d*lac*Δ(*lac*Z)M15) (22) was used for the production of monomeric supercoiled plasmid DNA for sequencing. CGTase (mutant) proteins were produced with the α-amylase and protease negative *Bacillus subtilis* strain DB104A (*amy npr*R2 *npr*E18 *apr*A3) (23). Plasmid pKM1 (Ap^r Km^r ColE1) (24) was digested with *Hin*cII. The fragment containing the kanamycin resistance marker was ligated with the largest fragment from plasmid pDP66S (25) containing the *B. circulans* strain 251 *cgt* gene digested with *Hin*dIII and *Xba*I (made blunt with Klenow polymerase). The resulting CGTase protein expression shuttle vector pDP66K, with the *cgt* gene under control of the erythromycin-inducible p32 promoter (26), was transformed to *E. coli* MC1061 under selection for erythromycin and kanamycin resistance (see Fig. 2). This plasmid was considerably more stable than plasmid pDP66S, both in *E. coli* and in *B. subtilis*. DNA manipulations and calcium chloride transformation of

* This work was financially supported by the Netherlands Programma Commissie voor Biotechnologie (PCB) of the Netherlands Ministry of Economic Affairs and the Groningen Biomolecular Sciences and Biotechnology Institute (GBB) and by grants of the Netherlands Ministry of Economic Affairs, the Ministry of Education, Culture and Science, the Ministry of Agriculture, Nature Management and Fisheries, and the Netherlands Organization for Scientific Research (NWO) in the framework of the biotechnology programme of the Association of Biotechnology Research Schools in the Netherlands (ABON). The costs of publication of this article were defrayed in part by the payment of page charges. This article must therefore be hereby marked "*advertisement*" in accordance with 18 U.S.C. Section 1734 solely to indicate this fact.

The atomic coordinates and structure factors (code 1TCM) have been deposited in the Protein Data Bank, Brookhaven National Laboratory, Upton, NY.

§ Contributed equally to this work.

‖ To whom correspondence should be addressed. Tel.: 31-50-3632150; Fax: 31-50-3632154; E-mail: L.Dijkhuizen@biol.rug.nl.

TABLE I
Data collection statistics and quality of the final model for the W616A mutant of CGTase

R_{merge} is defined as $R_{merge} = (\Sigma\Sigma|I_j(hkl) - \langle I(hkl)\rangle|)/(\Sigma\Sigma\langle I(hkl)\rangle)$, and the crystallographic R-factor is defined as $R = \Sigma||F_{obs}| - |F_{calc}||/\Sigma|F_{obs}|$. Free R factors were calculated using 5% of the unique reflections.

Cell dimensions ($P2_1$):	
a (Å)	73.7
b (Å)	84.8
c (Å)	118.3
β (degrees)	107.0
Resolution range (Å)	45.1–2.2
Total number of observations	133691
Number of discarded observations	717
Number of unique reflections	50563
R_{merge}	0.083
Completeness of data (%)	71.3
Completeness (%) of last	51.5
Resolution shell (Å)	(2.24–2.20)
Number of protein atoms	2 × 5255
Number of calcium atoms	2 × 2
Number of solvent sites[a]	119/144
Average B factor (Å^2)[a]	20.0/18.1
Final R factor/R-free (%)	19.3/25.0
Rms deviations from ideality for	
Bond lengths (Å)	0.005
Cell dimensions ($P2_1$):	
Bond angles (deg)	0.72
Torsion angles (deg)	20.1
Trigonal planes (Å)	0.007
Planar groups (Å)	0.010
van der Waals contacts (Å)	0.016
Rms difference in B for	
Neighboring atoms (Å^2)	1.98

[a] For molecule A and B, respectively.

E. coli strains were as described (27). Transformation of *B. subtilis* was performed according to Bron (28).

Site-directed Mutagenesis—Mutations were introduced with a PCR[1] method using VENT-DNA polymerase (New England Biolabs Inc., Beverly, MA). The first PCR reaction was carried out with a mutagenesis primer for the coding strand plus a primer 910-1050 bp downstream on the template strand. The 910-1050-bp reaction product was subsequently used as primer in a second PCR reaction together with a primer 760–900 bp upstream on the coding strand. The product of the last reaction (1800 bp) was cut with *Bgl*I and *Hin*dIII and exchanged with the corresponding fragment (600 bp) from the vector pDP66K. The resulting (mutant) plasmid was transformed to *E. coli* MC1061 cells. The following oligonucleotides were used to produce the mutations: Y633A, 5′-G GTC GTT TAC CAG GCG CCG AAC TGG-3′; W616A, 5′-GC GAG CTC GGG AAC GCG GAC CCG-3′; W662A, 5′-CC GTC ACC GCG GAA GGC GGC-3′. Successful mutagenesis resulted in the appearance of the underlined restriction sites, allowing rapid screening of potential mutants. For Y633A, this restriction site was *Nar*I, for W616A, it was *Sac*I, and for W662A, it was *Sac*II. A mutation frequency close to 70% was observed; all mutations were confirmed by restriction analysis and DNA sequencing.

DNA Sequencing—Plasmid pDP66K carrying the correct restriction site was transformed to *E. coli* DH5α cells. DNA sequence determination was performed on supercoiled plasmid DNA using the dideoxy chain termination method (29) and the T7 sequencing kit from Pharmacia Biotech Inc., Sweden.

Growth Conditions and Purification of CGTase Proteins—Plasmid carrying bacterial strains were grown on LB agar in the presence of the antibiotics erythromycin and kanamycin, at concentrations of 100 and 5 μg/ml for *E. coli* and *B. subtilis*, respectively (27). *B. subtilis* strain DB104A with plasmid pDP66K, carrying wild-type or mutant *cgt* genes, was grown in a 5-liter flask, containing 1 liter of medium with 2% trypton, 0.5% yeast extract, 1% sodium chloride, and 1% casamino acids, pH 7.0, with 10 μg/ml erythromycin and 5 μg/ml kanamycin, to a final optical density at 600 nm of 4.5 (for approximately 36 h). Under these conditions, high extracellular CGTase levels were obtained reproducibly, allowing purification to homogeneity of up to 25 mg of CGTase protein/liter. The culture was centrifuged at 4 °C for 30 min at 10,000 × *g*. The (mutant) CGTases in the culture supernatants were further purified to homogeneity by affinity chromatography, using a 30-ml α-cyclodextrin-Sepharose-6FF column (Pharmacia, Sweden) (30) with a maximal capacity of 3.5 mg protein/ml. After washing with 10 mM sodium acetate buffer, pH 5.5, bound CGTase was eluted with the same buffer containing 10 mg/ml α-cyclodextrin.

[1] The abbreviations used are: PCR, polymerase chain reaction; bp, base pairs; MBS, maltose binding sites.

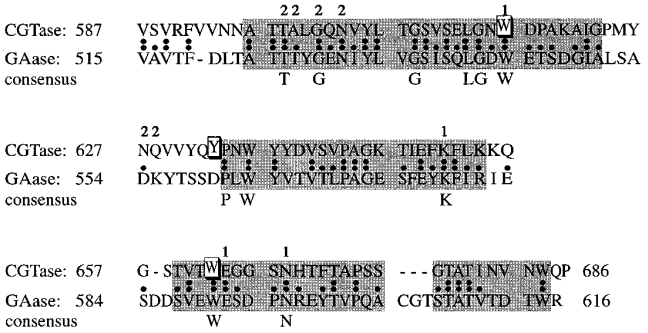

FIG. 1. **Alignment of the raw starch binding domains in *B. strain* 251 CGTase and *Aspergillus niger* glucoamylase (GAase) and the consensus raw starch binding motif (5, 9, 10).** Residues making hydrophobic interactions with a maltose molecule bound in MBS1 (Trp-616, Tr-662) or MBS2 (Tyr-633) of *B. circulans* CGTase are shown in a *box* (□); those making hydrogen bonds with a maltose molecule bound in MBS1 or MBS2 are indicated by number *1* and *2*, respectively (5). **:**, identical residues; **.**, similar residues.

Enzyme Assays—β-Cyclodextrin forming activity was determined by incubating appropriately diluted enzyme (0.1–0.2 units of activity) for 2–4 min at 50 °C. A 5% solution of partially hydrolyzed potato starch, with an average degree of polymerization of 50 (Paselli SA2; AVEBE, Foxhol, The Netherlands), was used as a substrate. At regular time intervals, samples were taken, and the amount of β-cyclodextrin formed was determined based on its ability to form a stable colorless inclusion complex with phenolphthalein (31). One unit of activity is defined as the amount of enzyme able to produce 1 μmol of β-cyclodextrin/min.

Raw Starch Binding Properties—Raw starch binding properties were studied by incubating pure (mutant) CGTase (6 μg/ml final concentration) with increasing amounts (0–10%) of granular potato starch (AVEBE) at 4 °C for 1 h in the presence and absence of 0.1 mM of β-cyclodextrin (equilibrium was reached within 10 min). CGTase protein bound to the starch granules was spun down at 4 °C for 1 min at 10,000 × *g*, and the remaining cyclization activity in the supernatant was measured as described above.

Kinetic studies were performed by measuring β-cyclodextrin forming activity of (mutant) CGTase enzymes (final concentration 0.6 μg/ml, equivalent to 0.15–0.18 units) at Paselli SA2 concentrations ranging from 0–5%, in the presence or absence of 1 or 2 mM of β-cyclodextrin. Alternatively, kinetic studies were performed by incubating CGTase enzymes (final concentration 6 μg/ml) for 10 min with raw starch concentrations ranging from 0–50%; β-cyclodextrin formation was determined as above. All experiments were carried out at least in triplicate. Plots of the data obtained (see Figs. 4–6) were better described with the Hill equation than the Michaelis-Menten equation, indicating that some form of cooperativity is involved both in the cyclization reaction and raw starch binding kinetics. To determine the degree of cooperativity, the data from these kinetic and binding studies were fitted with an equation equivalent to the Hill equation (Equation 1) (32), using the Sigma Plot program (Jandel Scientific). Plotting *x versus* [*S*] yields a sigmoidal curve (primary plot).

$$x = \frac{X_{max} \cdot [S]^h}{K_{50}{}^h + [S]^h} \qquad \text{(Eq. 1)}$$

In this equation, [*S*] is the substrate concentration; K_{50} is equivalent to the dissociation constant; h is the Hill constant, indicating the degree of cooperativity involved; x is for the binding studies where b is the fraction of protein bound to the raw starch, and for the kinetic studies where v is the velocity of the reaction; X_{max} is for the binding studies where B_{max} is the maximal fraction of protein bound to the raw starch, and for the kinetic studies where V_{max} is the maximal velocity of the reaction.

Equation 1 can be rewritten as follows.

$$\log\left(\frac{x}{X_{max} - x}\right) = h \cdot \log[S] - h \cdot \log K_{50} \qquad \text{(Eq. 2)}$$

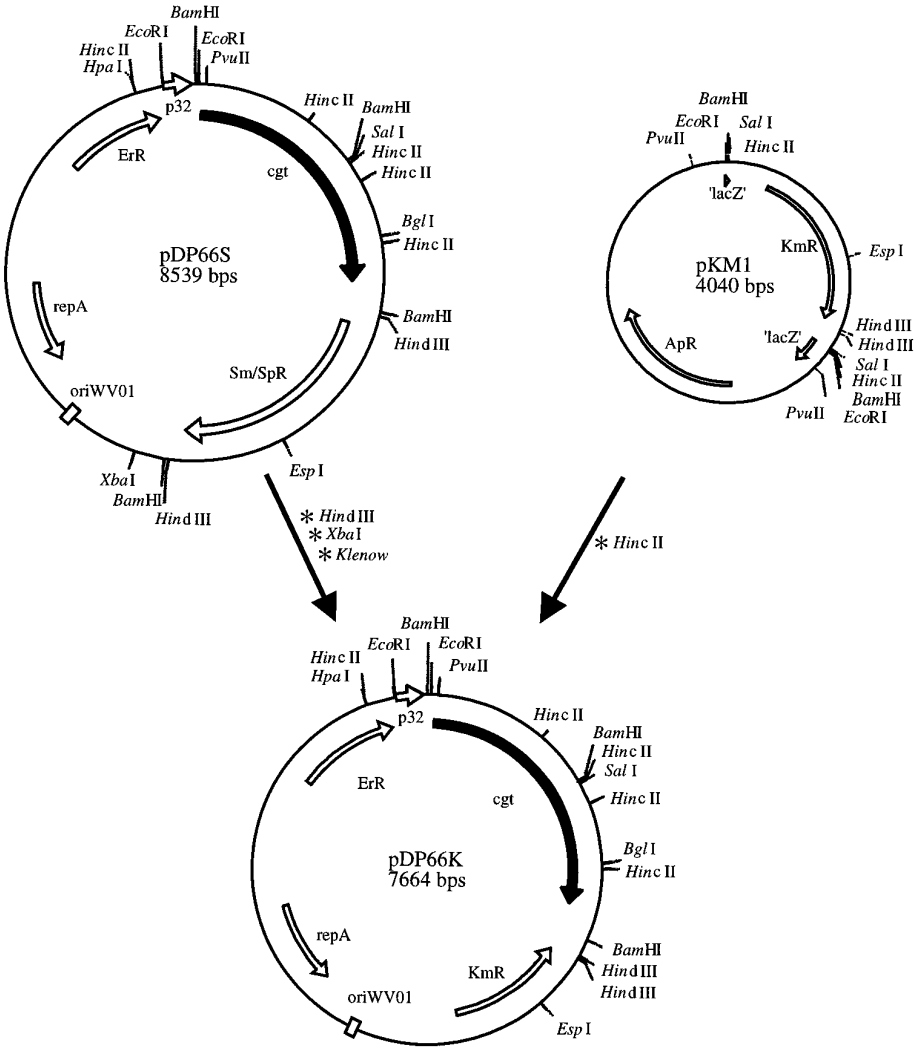

FIG. 2. **Construction of plasmid pDP66K.** Subcloning steps are indicated adjacent to the *arrows*.

By plotting $\log(x/X_{max\ -\ x})$ *versus* $\log[S]$ (Hill plot), a straight line is obtained (secondary plot). In this plot, the slope of the line gives the Hill constant h, the y intercept is $-h\cdot\log K_{50}$ and the x intercept is $\log K_{50}$. K_i values for the inhibitory effect of β-cyclodextrin on kinetics of the cyclization reaction on Paselli SA2 were calculated using the following equations (32).

For competitive inhibition

$$K_{i1} = \frac{[I]}{\frac{K_{50_i}}{K_{50}} - 1}. \quad \text{(Eq. 3)}$$

For non-competitive inhibition

$$K_{i2} = \frac{[I]}{\frac{V_{max}}{V_{max_i}} - 1}. \quad \text{(Eq. 4)}$$

In Equation 3, K_{50_i} is the apparent K_{50} when β-cyclodextrin is added, and K_{i1} is the concentration β-cyclodextrin at which the apparent K_{50} is $2\cdot K_{50}$. In Equation 4, V_{max_i} is the apparent V_{max} when β-cyclodextrin is added and K_{i2} is the concentration of β-cyclodextrin at which the apparent V_{max} is $1/20\cdot V_{max}$.

Crystallization and Data Collection—Attempts to crystallize the W616A mutant CGTase under similar conditions as the wild type (5) resulted in phase separation in the hanging drops. Therefore, a Sparse matrix (33) (48 experiments) was set up using hanging drops with a protein concentration of 8 mg/ml in 10 mM sodium acetate buffer, pH 5.5, at room temperature. Five conditions, all containing PEG8000 at pH 5.5–7.3, resulted in crystalline material. Refinement of these conditions showed that the biggest crystals could be grown from 9–12% (w/v) PEG8000 at pH 6.8 to 7.2. Many crystals were intergrown plates or twinned needles, but a small number of them were rod-shaped single crystals belonging to the monoclinic spacegroup $P2_1$ with cell dimensions a = 73.7 Å, b = 84.8 Å, c = 118.3 Å, and β = 107.0°. X-ray diffraction data were collected on a MacScience Dip2000K image plate system and processed with XDS (34) yielding a data set of 50,563 unique reflections with an R_{sym} of 8.3% and 71.3% completeness to 2.2 Å resolution.

Molecular Replacement—Molecular replacement was carried out with the native CGTase structure (without maltoses or solvent and with residue Trp-616 replaced by Ala) as the search model. The rotation and translation functions (35, 36) were solved with diffraction data in the 8.0–4.0 Å resolution range. Two unique solutions were obtained at 9σ, indicating the presence of a dimer in the asymmetric unit. The relative y coordinates of the two solutions were determined with the program BRUTE (37). The two solutions correspond to a rotation of the search model over α = 77.5°, β = 140.0°, and γ = 150.0° and a translation in fractional coordinates of 0.13, 0.00, and 0.24 for the first solution and a rotation of α = 105.0°, β = 100.0°, γ = 355.0° and a translation of 0.44, 0.44, and 0.03 for the second solution.

Structure Refinement—Both molecules were subjected to rigid body refinement with TNT (38), followed by alternating manual adjustments with O (39) and refinement with TNT. Free R-factors (40) were calculated using 5% of the data. The final model has crystallographic and free R-factors of 19.3 and 25.0%, respectively, and good stereochemistry (see Table I). The final model has been deposited at the protein databank (41) (entry code 1TCM).

RESULTS AND DISCUSSION

Structures of Maltose Binding Sites in the E-domain—In previous studies, we identified two maltose binding sites (MBS)

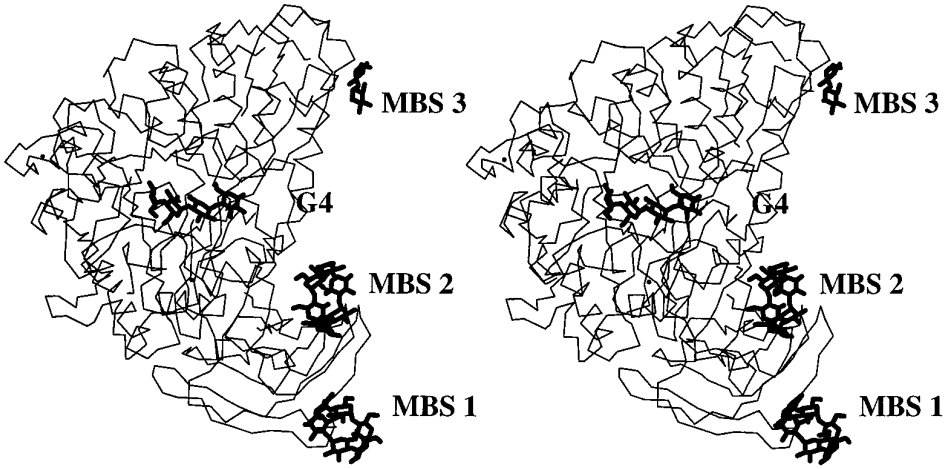

FIG. 3. **Stereo representation of α-cyclodextrin stacked over the hydrophobic residues of the maltose binding sites in the E-domain of *B. circulans* strain 251 CGTase.** Visible also are maltose stacked on maltose binding site three (*MBS3*) in the C-domain and maltotetraose (*G4*) in the active site (20).

in the E-domain of *B. circulans* strain 251 CGTase (5). MBS1 includes Trp-616 and Trp-662, which bind a maltose unit through van der Waals contacts of their indole groups with the glucose rings. Direct hydrogen bonds with the side groups of Lys-651 and Asn-667 and water-mediated hydrogen bonds with the main chain carbonyl oxygen atoms of Trp-616 and Glu-663 further enhance maltose binding (Fig. 1) (5). In MBS2, Tyr-633 forms van der Waals contacts with a glucose residue. Direct hydrogen bonds with the side chains of Thr-598, Asn-627, and Gln-628, the main chain carbonyl oxygen atoms of Ala-599 and Gly-601, and one water-mediated hydrogen bond with Asn-603 complete maltose binding (Fig. 1) (5). MBS2 is located near a groove leading to the active site (Fig. 3), indicating that its function may be a combination of starch binding and guiding the substrate into the groove leading to the active site. A third MBS, located at the C-domain, has also been identified (5). The distances between the different MBS sites measured over the surface of the protein are from MBS1 to MBS2, 30Å; from MBS1 to MBS3, 60Å; and from MBS2 to MBS3, 52Å (± 5Å). Recently, we showed that cyclodextrins bind at MBS1 and MBS2 but not (or less) at MBS3 (Fig. 3) (20). The functions of MBS1 and MBS2 in the E-domain were studied further by replacing the residues responsible for hydrophobic interactions with sugar residues (Trp-616, Tyr-633, and Trp-662) by alanine residues. The biochemical and structural properties of these mutant CGTase proteins are reported below.

MBS1 (Trp-616, Trp-662) Is Most Important for the Raw Starch Binding Capacity—The wild-type protein has a high affinity toward raw starch, and at high substrate concentration, virtually all of the enzyme is bound to the raw starch (Fig. 4(*A1*) and Table II). Especially, the W616A/W662A mutations in MBS1 clearly affected raw starch binding, resulting in highly decreased affinities as shown by the strongly enhanced K_{50} (dissociation constant) values (Fig. 4(*B*) and Table II). TheY633A mutation in MBS2 also resulted in a strong increase of the K_{50} value (Fig. 4(*C*) and Table II). The W616A and W616A/W662A mutations also resulted in a decreased binding capacity indicated by the strongly reduced B_{max} (maximal fraction of bound protein) values (Fig. 4(*B1*) and Table II). The Y633A mutation had much less effect on B_{max} values (Fig. 4(*C1*) and Table II). From this, we conclude that MBS1 (Trp-616, Trp-662) is of crucial importance for raw starch binding, while MBS2 (Tyr-633) especially improves the binding affinity for raw starch and only makes a relatively small contribution to the binding capacity.

The Hill factor *h* (the degree of cooperativity) for raw starch

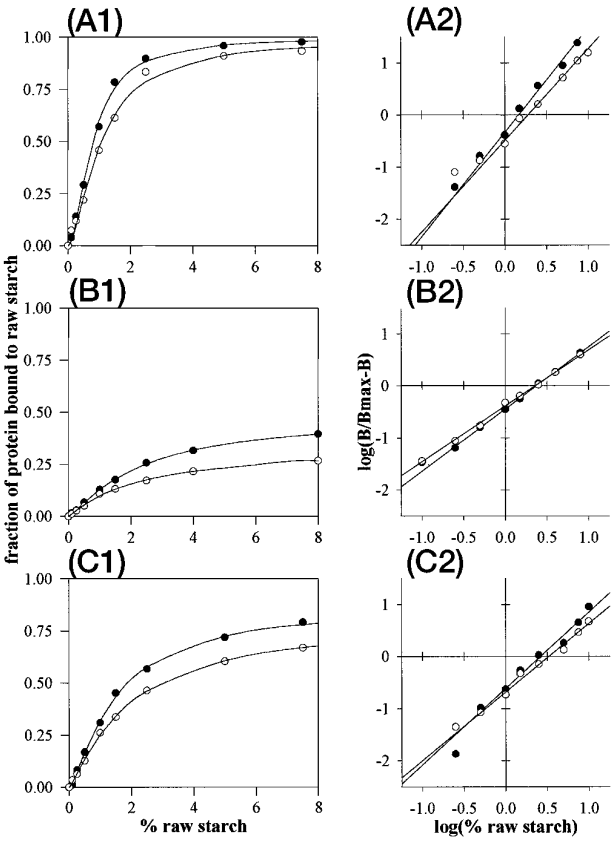

FIG. 4. **Primary plots (A-, B-, or C1) and Hill plots (A-, B-, or C2) for binding to raw starch of *B. circulans* strain 251 wild type (*A*), W616A/W662A (*B*), and Y633A (*C*) mutant CGTase enzymes in the presence of 0.1 mM[r (○) and 0 mM (●) β-cyclodextrin.**

binding is 1.7 for the wild-type CGTase, indicating that at least two sites are involved in binding (Table II). The Hill factors have severely decreased in mutants W616A and W616A/W662A, demonstrating that in wild-type CGTase MBS1 is one of the sites contributing to cooperative binding. Mutant Y633A has an intermediate Hill factor; cooperativity in raw starch binding thus was less affected in this mutant. This suggests that one or more sites other than MBS2 cooperate with MBS1 in raw starch binding in wild-type CGTase. This is in agreement with the residual starch binding occurring in the W616A/W662A mutant. Conceivably, these alternative sites are the

TABLE II
Binding properties of B. circulans strain 251 wild type and mutant CGTase proteins with raw starch (RS): effects of β-cyclodextrin (CD)

(Mutant) protein	B_{max}		K_{50} (% RS)		h	
	0 mM β-CD	0.1 mM β-CD	0 mM β-CD	0.1 mM β-CD	0 mM β-CD	0.1 mM β-CD
Wild type	1.00 ± 0.02	0.99 ± 0.03	0.79 ± 0.03	1.06 ± 0.07	1.78 ± 0.11	1.56 ± 0.14
W616A	0.63 ± 0.03	0.42 ± 0.02	1.56 ± 0.21	1.30 ± 0.15	1.05 ± 0.09	1.41 ± 0.18
W616A/W662A	0.49 ± 0.01	0.33 ± 0.02	2.36 ± 0.13	2.27 ± 0.30	1.19 ± 0.06	1.07 ± 0.07
Y633A	0.88 ± 0.02	0.81 ± 0.02	1.52 ± 0.07	1.97 ± 0.09	1.30 ± 0.06	1.17 ± 0.04

active site cleft and/or MBS3 in the C-domain. Preliminary results with an MBS3 mutant indicate that this site is indeed involved in raw starch binding (not shown).

β-Cyclodextrin Competitively Inhibits Raw Starch Binding at MBS1—Under cyclodextrin production conditions, *B. circulans* strain 251 CGTase suffers from product inhibition (19). A crystallographic analysis of cyclodextrin binding to CGTase revealed that cyclodextrin is bound at MBS1 and MBS2 (20) in the E-domain (Fig. 3), but not at MBS3 in the C-domain, or in the active site. We have now observed that the presence of β-cyclodextrin indeed affected the raw starch binding properties of the wild-type CGTase (Fig. 4(*A*) and Table II). Addition of β-cyclodextrin resulted in an unchanged raw starch binding capacity (indicated by B_{max}) but in an increased K_{50} (dissociation constant) value for the wild-type CGTase, reflecting a decreased affinity for raw starch. β-Cyclodextrin thus competitively inhibits raw starch binding by the wild-type enzyme. Almost the same competitive effect was observed for mutant Y633A (Fig. 4(*C*) and Table II), indicating that with an impaired MBS2, the effect of β-cyclodextrin on raw starch binding had not changed. This again illustrates that MBS2 does not contribute substantially to raw starch binding. The effect of β-cyclodextrin on the binding of raw starch by mutants W616A and W616A/W662A, however, was completely different. Here the K_{50} values did not change upon addition of β-cyclodextrin (Fig. 4(*B2*) and Table II), while the raw starch binding capacity (indicated by B_{max}) was severely decreased (Fig. 4(*B1*) and Table II). β-Cyclodextrin, thus, non-competitively inhibits raw starch binding by CGTase mutants with an impaired MBS1. It follows that in the wild-type CGTase, binding competition between raw starch and β-cyclodextrin takes place at MBS1.

MBS2 (Tyr-633) Is Most Important for Guiding Linear Starch Chains into the Active Site—The raw starch binding studies show that MBS1 is important for the binding capacity, while MBS2 enhances the affinity, suggesting that these sites have distinct functions. Kinetic studies of the cyclization activity of (mutant) CGTase proteins with soluble starch (Paselli SA2) as substrate were performed to further elucidate these functions (Fig. 5 and Table III). Mutations in MBS1 and MBS2 had relatively minor effects on the V_{max} (maximal velocity of the reaction) values. The mutations W616A/W662A in MBS1 resulted in a doubling of the K_{50} (dissociation constant) value (Table III), indicating that binding of the substrate at MBS1 on the E-domain enhances the affinity of the enzyme for the substrate. Although MBS2 does not strongly contribute to raw starch binding capacity, mutation Y633A resulted in an even more increased K_{50} value (Table III), indicating a strongly reduced affinity for the substrate. This, together with the fact that MBS2 is situated at the beginning of the groove leading to the active site (Fig. 3), suggests a role for MBS2 in guiding the substrate to the active site. The cooperativity factor h decreased to 1 for all mutants, indicating complete loss of cooperativity (Table III). This implies that both MBS1 and MBS2 are crucial for the cooperativity observed in cyclization reaction kinetics on Paselli SA2. In the absence of MBS1, the affinity of MBS2 for the substrate is very low (Table II), causing a reduced efficiency of this MBS2; furthermore, MBS2 and the active site

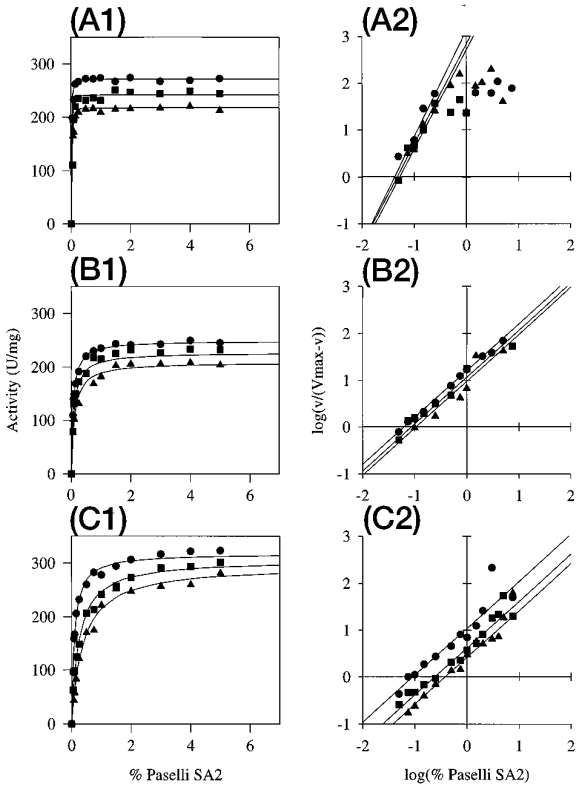

FIG. 5. **Primary plots (A-, B-, or C1) and Hill plots (A-, B-, or C2) for the reaction kinetics on Paselli SA2 (soluble starch) of *B. circulans* strain 251 wild type (*A*), W616A/W662A (*B*), and Y633A (*C*) mutant CGTase enzymes in the presence of 2 mM (▲), 1 mM (■), and 0 mM (●) β-cyclodextrin.** The seemingly random distribution of points at high Paselli SA2 concentrations (*A2*) are caused by the low K_{50} and high h values for the wild-type enzyme.

cleft can be regarded as one binding site for a high molecular substrate. In the absence of MBS2 the substrate will still bind to MBS1, but it is not efficiently guided to the active site.

β-Cyclodextrin Inhibits the Cyclization Reaction at the Active Site and by Interfering with MBS2—β-Cyclodextrin reduces the capacity of CGTase to bind raw starch (Table II). Also, the cyclization reaction with soluble starch is inhibited by β-cyclodextrin (Table III). This inhibitory effect on the cyclization reaction was investigated further to see whether it involves the maltose binding sites. For the wild-type enzyme, the presence of β-cyclodextrin resulted in clearly decreased V_{max} and increased K_{50} values (Fig. 5(*A*) and Table III). Inhibition of cyclization activity by β-cyclodextrin, therefore, appears to be of a mixed type (32). This type of inhibition can be divided into an effect on the K_{50} normally observed for competitive inhibition, yielding K_{i1}, and an effect on the V_{max} normally observed for non-competitive inhibition, yielding K_{i2} (Table III). So in the wild type, β-cyclodextrin interferes competitively with the cyclization reaction at the active site and non-competitively elsewhere on the enzyme. The W616A and W616A/W662A mutants showed the same type of inhibition as the wild type, with K_i

TABLE III
Kinetic properties of the cyclization reaction of B. circulans strain 251 wild type and mutant CGTase proteins with Paselli SA2; effects of β-cyclodextrin (CD)

(Mutant) protein	V_{max}	K_{50}	h	K_{i1}[a]	K_{i2}[b]
	units/mg	*mM*		*mM*	*mM*
Wild type	271.2 ± 1.7	0.028 ± 0.003	2.3 ± 0.6	1.35 ± 0.59	8.1 ± 1.0
W616A	251.0 ± 3.2	0.037 ± 0.005	[c]	0.84 ± 0.31	11.5 ± 1.8
W616A/W662A	248.8 ± 3.7	0.062 ± 0.006	[c]	1.95 ± 0.51	10.4 ± 1.6
Y633A	319.0 ± 5.7	0.092 ± 0.010	[c]	0.58 ± 0.07	27.8 ± 9.7

[a] K_{i1} represents competitive inhibition.
[b] K_{i2} represents non-competitive inhibition.
[c] Fitting of these data was performed using the Michaelis-Menten equation (h = 1).

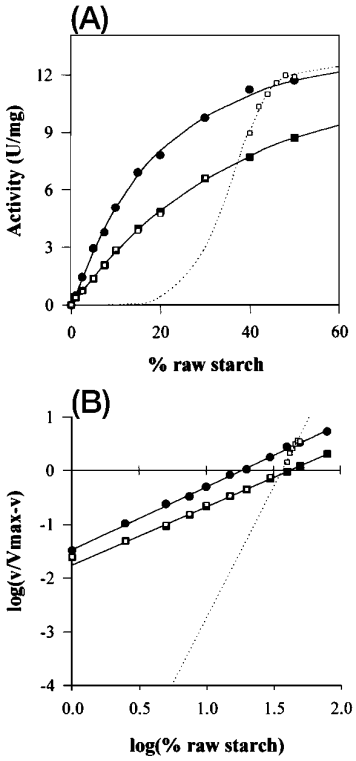

FIG. 6. **Primary plots (*A*) and Hill plots (*B*) for the reaction kinetics on raw starch of *B. circulans* strain 251 wild type (●), W616A/W662A (□), and Y633A (■) mutant CGTase enzymes.** The *dotted line* indicates the modeled curve resulting from the supposed interaction between MBS2 (E-domain) and MBS3 (C-domain).

values for β-cyclodextrin, which did not differ significantly from the wild-type values (Table III). Upon addition of β-cyclodextrin, the Y633A V_{max}, however, was less affected, resulting in a higher K_{i2}, while its K_{50} value increased more, resulting in a lower K_{i1} (Fig. 5(*C*) and Table III). This indicates that in wild-type CGTase, non-competitive inhibition is mainly caused by interference of β-cyclodextrin with the function of MBS2. A β-cyclodextrin bound to this site may not only prevent starch binding but also block the groove leading to the active site (Fig. 3) (5, 20). The more pronounced competitive type of inhibition of the cyclization reaction in the Y633A mutant is probably a direct effect of the decreased non-competitive inhibition; the relatively higher V_{max}, upon addition of β-cyclodextrin compared with the wild-type and other mutant enzymes, automatically results in a higher K_{50}.

The raw starch binding studies showed that MBS1 (Trp-616, Trp-662) is crucial for raw starch binding, while the kinetic studies of cyclization activity on Paselli SA2 clarified that MBS2 (Tyr-633) has a function in guiding linear starch chains into the active site.

The Functions of MBS1 and MBS2 Are Equally Important for Cyclization Activity with Raw Starch—The cyclization reaction kinetics was also studied with raw starch as substrate (Fig. 6 and Table IV). Mutations W616A (MBS1) and Y633A (MBS2) resulted in increased K50 (dissociation constant) values, while V_{max} (maximal velocity of the reaction) values remained unaffected (Table IV). The kinetic parameters of the W616A/W662A mutant could not be measured accurately because of a shift in the curve (Fig. 6); most likely, its V_{max} approaches those of wild type and the W616A and Y633A CGTases, and its K_{50} value approaches those of mutants W616A and Y633A. The results nevertheless clearly indicate that the affinity toward raw starch in the cyclization reaction is much higher when both MBS1 and MBS2 are present (Fig. 6). The Y633A mutation resulted in a similarly reduced affinity for raw starch (Table IV) and Paselli SA2 (Table III) when studying the cyclization reaction kinetics. As discussed above, loss of MBS2 converts CGTase into a protein that is less efficient in guiding the starch chain to the active site, while loss of MBS1 results in a reduced ability to bind to raw starch granules. For the conversion of raw starch into cyclodextrins, both these features of the two maltose binding sites are equally important. At the surface of starch granules, chains of varying lengths may protrude into the medium. Binding of CGTase protein to a starch granule will result in an increased local concentration of substrate for the enzyme. Loss of binding, therefore, results in a decrease in the effective substrate concentration, and thus in an increased K_{50} value. Fig. 6 shows that, up to a concentration of 35% raw starch, mutations in both MBS1 and MBS2 appear to have similar effects. At higher raw starch concentrations, however, the cyclization activity of the W616A/W662A mutant (MBS1) shifts toward the level displayed by wild type. This shift in the curve suggests that MBS1 is functionally replaced by another binding site. Conceivably, this site is MBS3 in the C-domain, also involved in raw starch binding. This effect may only be visible at high raw starch concentrations because of the relatively long distance between MBS3 and MBS2, which might cause a high Hill factor value (Fig. 6(*B*), (hypothetical) *dotted line*). Starch chains of sufficient length may be scarce on the surface of the starch granule, resulting in a high K_{50} value (Fig. 6(*A*), (hypothetical) *dotted curve*).

TABLE IV
Kinetic properties of the cyclization reaction of B. circulans strain 251 wild type and mutant CGTase proteins with raw starch

(Mutant) protein	V_{max}	K_{50}
	units/mg	*% RS*
Wild type	15.3 ± 0.5	18.4 ± 1.3
W616A	14.4 ± 2.1	43.3 ± 11.4
W616A/W662A	(15.3)	(42.5)
Y633A	16.0 ± 0.5	42.5 ± 2.7

Crystal Structure of the W616A Mutant CGTase—In wild-type CGTase, the maltose that is bound to MBS1 is involved in crystal packing contacts (5). Replacement of Trp-616 by Ala reduced the affinity for binding of carbohydrate chains at this site. This has resulted in a novel maltose-independent crystal

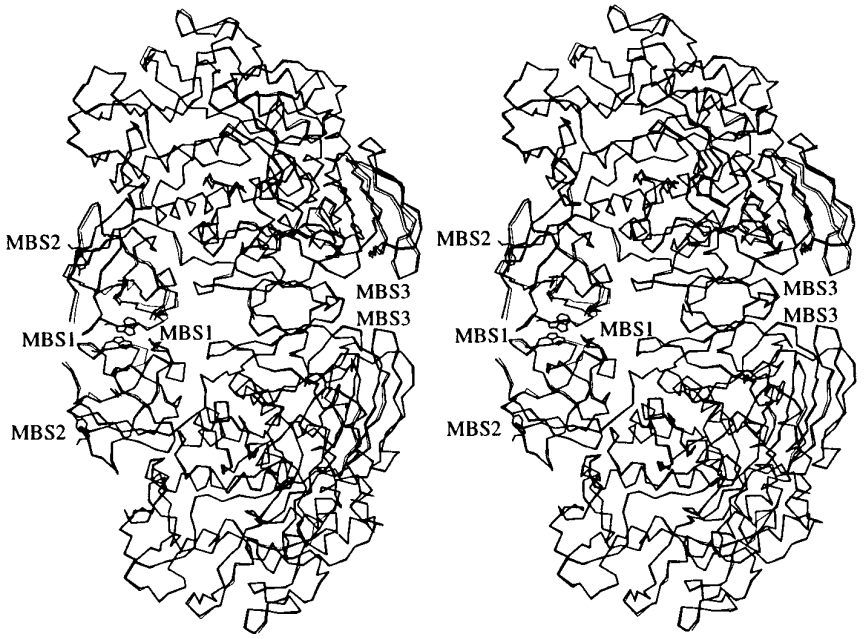

FIG. 7. **Stereo view of the C_α-trace of the crystallographic dimer of the W616A mutant of CGTase from *B. circulans* strain 251.** The W616A mutant is drawn with *thick lines* while the superimposed wild-type enzyme structure is drawn in *thin lines*. The maltose binding sites and the corresponding aromatic residues have been indicated. The W616A structure deviates only from the wild-type at regions near crystal contacts and the dimer interface.

TABLE V

Inter-molecular hydrogen bonds and van der Waals interactions of the W616A CGTase mutant

For van der Waals interactions, only the shortest distance between two residues is listed. Symmetry operation 1 denotes contacts within the dimer.

van der Waals interactions		Distance		Hydrogen bonds		Distance	
Atom 1	Atom 2	(Å)	Symop[a]	Atom 1	Atom 2	(Å)	Symop[a]
Trp A662-Cη2	Trp B662-Cδ1	3.0	1	Ala A616-O	Trp B662-Nϵ1	3.0	1
Phe A39-Cϵ2	Tyr A301-Cϵ2	3.6	2	Asp A617-Oδ1	Asp B617-Oδ1	3.0	1
Gly A41-Cα	Tyr A301-Cϵ2	3.5	2	Trp A662-N	Gly B665-O	2.7	1
Asp B147-Cβ	Val B265-Cγ2	3.5	3	Trp A662-O	Gly B665-N	3.3	1
				Asp A147-O	Tyr A492-OH	3.0	4
				Ser A205-Oγ	Gln B453-O	3.4	4
				Thr A206-Oγ1	Gln B453-Nϵ2	2.8	4
				Asn A336-Oδ1	Ser A658-Oγ	2.9	2
				Ala A557-N	Ser B90-Oγ	3.3	5
				Asn A681-O	Cys B400-Sγ	2.8	4
				Pro A686-O	Lys B128-Nζ	3.3	4
				Tyr B301-OH	Gln B632-Oϵ1	3.1	5
				Asn B416-Oδ1	Gln B632-Nϵ2	3.3	5
				Asn B416-Nδ2	Gln B632-Oϵ1	2.8	5

[a] Symop, Symmetry operations are 1 = X, Y, Z; 2 = $1 - X, Y + 0.5, 1 - Z$; 3 = $1 \pm X, Y - 0.5, -Z$; 4 = $X - 1, Y, Z$; 5 = $1 - X, Y + 0.5, -Z$.

form. The W616A mutant CGTase crystallizes as a dimer with the mutated MBS1 of each monomer face to face (Fig. 7). Dynamic light scattering measurements of the protein dissolved in 10 mg/ml α-cyclodextrin and 10 mM sodium acetate, pH 5.5, showed, however, that the protein is monomeric in solution (results not shown) and that, therefore, the dimeric form is a crystallographic artifact. The two protein molecules in the dimer, called A and B, respectively, are related to each other by a rotation of 170° resulting in different local environments of the two molecules. The largest changes in the protein backbone conformation occur at residues A336–A338, A665–A659, B40–B43, B89–B91, B598–B603, and B655–B659, all of which are located at the surface of the protein, near the dimer interface or crystal packing contacts. The dimer interface is mainly polar, with the exception of a stacking interaction between the indole groups of Trp A662 and Trp B662. A summary of direct hydrogen bonds and hydrophobic interactions at crystal contacts and within the dimer interface is presented in Table V. Electron density in σ_a-weighted $2|F_o - F_c|$ maps (42) at position 616 in both monomers (Fig. 8) confirms that the Trp-616 to Ala mutation has been successful. In conclusion, the crystal structure of the W616A mutant CGTase shows that the mutation at MBS1 does not induce large structural changes in the overall fold of the protein but merely influences crystal packing due to the altered sugar binding capacity of the enzyme. The modified starch binding and cyclization kinetic properties observed with the mutant CGTase proteins thus are not due to conformational changes but can be directly related to the amino acid replacements.

CONCLUSIONS

Our data suggest the following functions for the maltose binding sites in the *B. circulans* strain 251 CGTase E-domain. MBS1 (with Trp-616, Trp-662) is required for efficient binding to raw starch granules with a minor contribution from MBS2 (with Tyr-633) and a major contribution from an additional binding site, probably MBS3 (with Trp-413, in the C-domain). A β-cyclodextrin bound at MBS1 competitively inhibits binding of CGTase to raw starch granules. The cyclization reaction kinetics with soluble starch indicated that MBS2 has an important role in guiding linear starch chains to the active site. For wild-type CGTase, a mixed type of inhibition by β-cyclodextrin was observed. Competitive inhibition takes place at the active site, while non-competitive inhibition results from interference of β-cyclodextrin with substrate binding at MBS2. β-Cyclodextrin bound at MBS2 may block the groove leading to

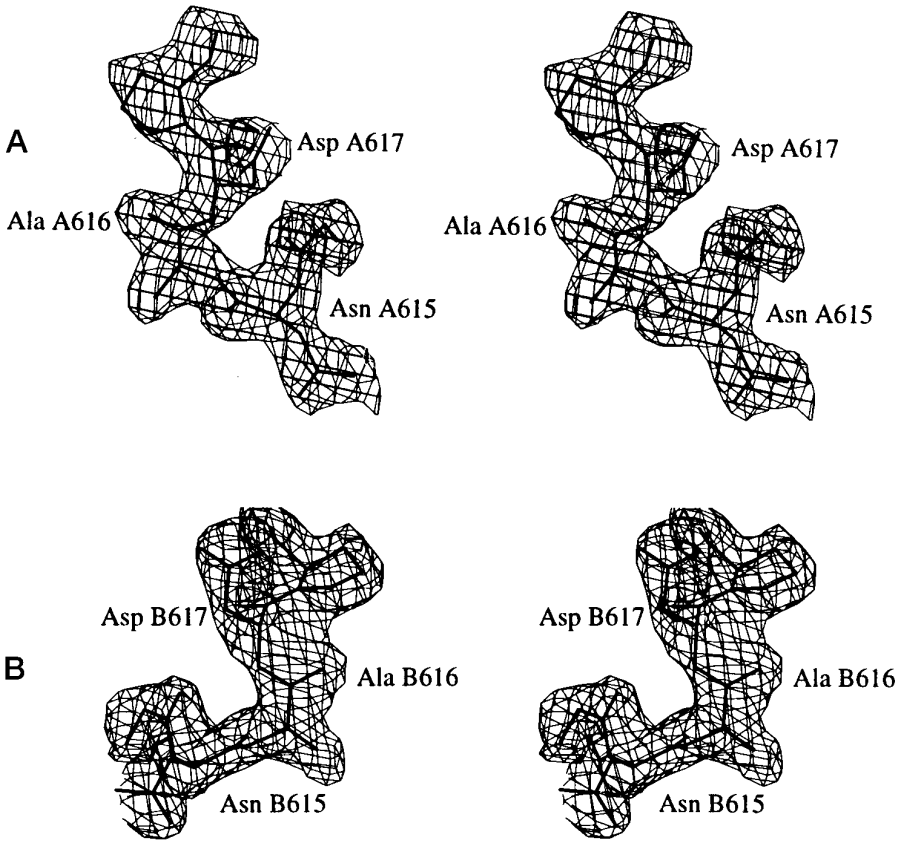

FIG. 8. **Electron density in $2|F_o - F_c|$ maps contoured at 1σ for residues A614–A618 and B614–B618, labeled *A* and *B*, respectively.** Residues adjacent to the mutated tryptophan have been indicated. The replacement of Trp-616 by Ala is confirmed by the electron density in this region.

the active site. The cyclization reaction kinetics with raw starch revealed that these different roles of MBS1 and MBS2 are equally important for degradation of raw starch.

Structural analysis of the W616A mutant CGTase revealed only minor changes compared with the wild-type enzyme. The modified starch binding and cyclization kinetic properties observed with the mutant CGTase proteins thus can be directly related to the amino acid replacements.

The data obtained on the functions of the CGTase E-domain in raw starch binding have important implications for our understanding of this process in glucoamylase and other members of the α-amylase family (9–12, 16, 43–45).

REFERENCES

1. Lawson, C. L., Bergsma, J., Bruinenberg, P., de Vries, G., Dijkhuizen, L., and Dijkstra, B. W. (1990) *J. Mol. Biol.* **214,** 807–809
2. French, D. (1957) *Adv. Carbohydr. Chem. Biochem.* **12,** 189–260
3. Saenger, W. (1980) *Angew. Chem. Int. Ed. Engl.* **19,** 344–362
4. Schmid, G. (1989) *Tibtech* **7,** 244–248
5. Lawson, C. L., van Montfort, R., Strokopytov, B., Rozeboom, H. J., Kalk, K. H., de Vries, G. E., Penninga, D., Dijkhuizen, L., and Dijkstra, B. W. (1994) *J. Mol. Biol.* **236,** 590–600
6. Hofmann, B. E., Bender, H., and Schulz, G. E. (1989) *J. Mol. Biol.* **209,** 793–800
7. Klein, C., and Schulz, G. E. (1991) *J. Mol. Biol.* **217,** 737–750
8. Kubota, M., Matsuura, Y., Sakai, S., and Katsube, Y. (1991) *Denpun Kagaku* **38,** 141–146
9. Svensson, B. (1989) *Biochem. J.* **264,** 309–311
10. Jespersen, H. M., Macgregor, E. A., Sierks, M. R., and Svensson, B. (1991) *J. Biochem. (Tokyo)* **280,** 51–55
11. Dalmia, B. K., and Nikolov, Z. L. (1991) *Enzyme Microb. Technol.* **13,** 982–990
12. Svensson, B., Clarke, A. J., and Svendsen, I. (1986) *Carlsburg Res. Commun* **51,** 61–73
13. Belshaw, N. J., and Williamson, G. (1993) *Eur. J. Biochem.* **211,** 717–724
14. Svensson, B., and Sierks, M. R. (1992) *Carbohydr. Res.* **227,** 29–44
15. Kusnadi, A. R., Chang, H. Y., Nikolov, Z. L., Metzler, D. E., and Metzler, C. M. (1994) *Ann. N. Y. Acad. Sci.* **721,** 168–177
16. Fagerstrom, R. (1994) *Microbiology* **140,** 2399–2407
17. Villette, J. R., Krzewinski, F. S., Looten, P. J., Sicard, P. J., and Bouquelet, S. J. L. (1992) *Biotechnol. Appl. Biochem.* **16,** 57–63
18. Dalmia, B. K., Schutte, K., and Nikolov, Z. L. (1995) *Biotechnol. Bioeng. Symp.* **47,** 575–584
19. Bergsma, J., Bruinenberg, P. M., Hokse, H., and Meiberg, J. M. B. (1988) in *Proceedings of the 4th Int. Symp. on Cyclodextrins* (Huber, O., and Szejtli, J. eds) pp. 41–46, Kluwer Academic Publishers, Dordrecht, The Netherlands
20. Knegtel, R. M. A., Strokopytov, B., Penninga, D., Faber, O. G., Rozeboom, H. J., Kalk, K. H., Dijkhuizen, L., and Dijkstra, B. W. (1995) *J. Biol. Chem.* **270,** 29256–29264
21. Meissner, P. S., Sisk, W. P., and Berman, M. L. (1987) *Proc. Natl. Acad. Sci. U. S. A.* **84,** 4171–4175
22. Hanahan, D. (1983) *J. Mol. Biol.* **166,** 557–580
23. Smith, H., de Jong, A., Bron, S., and Venema, G. (1988) *Gene* **70,** 351–361
24. Kiel, J. A. K. W., Vossen, J. P. M. J., and Venema, G. (1987) *Mol. & Gen. Genet.* **207,** 294–301
25. Penninga, D., Strokopytov, B., Rozeboom, H. J., Lawson, C. L., Dijkstra, B. W., Bergsma, J., and Dijkhuizen, L. (1995) *Biochemistry* **34,** 3368–3376
26. van de Vossen, J. M. B. M., Kodde, J., Haandrikman, A. J., Venema, G., and Kok, J. (1992) *Appl. Environ. Microbiol.* **58,** 3142–3149
27. Sambrook, J., Fritsch, E. F., and Maniatis, T. (1989) *Molecular Cloning: A Laboratory Manual*, Cold Spring Harbor Laboratory, New York
28. Bron, S. (1990) in *Modern Microbiological Methods for Bacillus* (Harwood, C. R., and Cutting, S. M., eds) pp. 146–147, John Wiley & Sons, New York/Chichester
29. Sanger, F., and Coulson, A. R. (1975) *J. Mol. Biol.* **94,** 441–448
30. Sundberg, L., and Porath, J. (1974) *J. Chromatogr.* **90,** 87–98
31. Vikmon, M. (1982) in *First Int. Symp. on Cyclodextrins, Budapest* (Szejtli, J., ed) pp. 69–74, D. Reidel Publishing, Dordrecht, The Netherlands
32. Creighton, T. E. (1993) *Proteins, Structures, and Molecular Properties*, pp. 329–461, W. H. Freeman and Company, New York
33. Jancarick, J., and Kim, S. H. (1991) *J. Appl. Crystallogr.* **24,** 409–411
34. Kabsch, W. J. (1993) *J. Appl. Crystallogr.* **26,** 795–800
35. Crowther, R. A. (1972) in *The Molecular Replacement Method* (Rossman, M. G., ed) pp. 173–178, Gordon and Breach, New York
36. Crowther, R. A., and Blow, D. M. (1967) *Acta Crystallogr.* **23,** 544–548
37. Fujinaga, M., and Read, R. J. (1987) *J. Appl. Crystallogr.* **20,** 517–521
38. Tronrud, D. E., Ten Eyck, L. F., and Matthews, B. W. (1987) *Acta Crystallogr. A* **43,** 489–501
39. Jones, T. A., Zou, J. Y., Cowan, S. W., and Kjeldgaard, M. (1991) *Acta Crystallogr. A* **47,** 110–119
40. Brünger, A. T. (1993) *Acta Crystallogr. D* **49,** 24–36
41. Bernstein, F. C., Koetzle, T. F., Williams, G. J. B., Meyer, E. F., Jr., Brice, M. D., Rodgers, J. R., Kennard, O., Shimanouchi, T., and Tasumi, M. (1977) *J. Mol. Biol.* **112,** 535–542
42. Read, R. J. (1986) *Acta Crystallogr. A* **42,** 140–149
43. Sigurskjold, B. W., Svensson, B., Williamson, G., and Driguez, H. (1994) *Eur. J. Biochem.* **225,** 133–141
44. Svensson, B., Larsen, K., and Gunnarsson, A. (1986) *J. Biochem.* **154,** 497–502
45. Chen, L., Ford, C., and Nikolov, Z. (1991) *Gene* **99,** 121–126